JACS
JOURNAL OF THE AMERICAN CHEMICAL SOCIETY
Article
pubs.acs.org/JACS

Au-Catalyzed Biaryl Coupling To Generate 5- to 9-Membered Rings: Turnover-Limiting Reductive Elimination versus π-Complexation

Tom J. A. Corrie,[†] Liam T. Ball,[†,§] Christopher A. Russell,[§] and Guy C. Lloyd-Jones*[,†]

[†]EaStChem, University of Edinburgh, Joseph Black Building, David Brewster Road, Edinburgh EH9 3FJ, U.K.
[§]School of Chemistry, University of Bristol, Cantock's Close, Bristol BS8 1TS, U.K.

Supporting Information

ABSTRACT: The intramolecular gold-catalyzed arylation of arenes by aryl-trimethylsilanes has been investigated from both mechanistic and preparative aspects. The reaction generates 5- to 9-membered rings, and of the 44 examples studied, 10 include a heteroatom (N, O). Tethering of the arene to the arylsilane provides not only a tool to probe the impact of the conformational flexibility of Ar−Au−Ar intermediates, via systematic modulation of the length of aryl−aryl linkage, but also the ability to arylate neutral and electron-poor arenes—substrates that do not react at all in the intermolecular process. Rendering the arylation intramolecular also results in phenomenologically simpler reaction kinetics, and overall these features have facilitated a detailed study of linear free energy relationships, kinetic isotope effects, and the first quantitative experimental data on the effects of aryl electron demand and conformational freedom on the rate of reductive elimination from diaryl-gold(III) species. The turnover-limiting step for the formation of a series of fluorene derivatives is sensitive to the reactivity of the arene and changes from reductive elimination to π-complexation for arenes bearing strongly electron-withdrawing substituents ($\sigma > 0.43$). Reductive elimination is accelerated by electron-donating substituents ($\rho = -2.0$) on one or both rings, with the individual σ-values being additive in nature. Longer and more flexible tethers between the two aryl rings result in faster reductive elimination from Ar−Au(X)−Ar and lead to the π-complexation of the arene by Ar−AuX_2 becoming the turnover-limiting step.

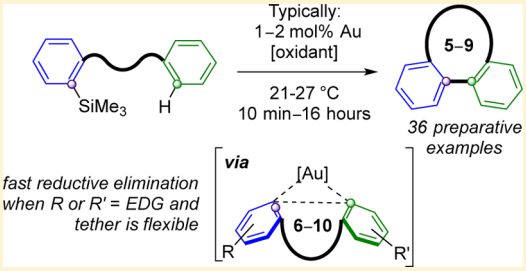

INTRODUCTION

Transition-metal-catalyzed cross-coupling has revolutionized synthesis,[1] with the biaryl motif a major focal point for research in this area.[2] The union of aryl-(pseudo)halides and aryl-metallic reagents has been extensively studied, and there is now substantial interest in more step- and atom-economic variants. In this regard, the reaction of arenes with aryl-metallic reagents, one class of the so-called "direct arylation" reaction, has received significant attention.[3] Catalysis by gold is emerging as a powerful synthetic tool.[4] We recently reported a gold-catalyzed *intermolecular* arylation of electron-rich arenes by aryl-trimethylsilanes (Scheme 1).[5]

The process is operationally simple and proceeds under air, often at room temperature, at low catalyst loadings (1−2 mol %), and with broad functional-group tolerance. In subsequent developments, Itami and Sagewa demonstrated that pyridylidene Au complexation facilitates arylation of isoxazoles, indoles, and benzothiophenes,[6] Jeon applied Au-catalyzed arylation to functionalize *ortho*-silyl aryl triflates generated via Rh/Ir-catalyzed traceless *ortho*-CH silation,[7] and we reported that silane and oxidant modification allows arylation of a range of heterocycles.[8]

Major advances have also been made toward understanding the unique reactivity and selectivity of catalytic reactions proceeding via Au(I) and Au(III) intermediates.[6,9] Nonetheless, in comparison to many transition-metal-catalyzed processes, mechanistic understanding of homogeneous gold catalysis remains less well developed. In 2014, we reported our initial mechanistic investigations into the gold-catalyzed *intermolecular* arylation (Scheme 1).[9h] Study of the precatalyst activation process revealed that, during an approximately 2 h induction period, the Au(I)-phosphine complex was oxidized to yield PPh_3O and the active gold catalyst: a solvated AuX_3 species (X = CSA, OTs). By changing to a $thtAuBr_3$ precatalyst (tht = tetrahydrothiophene), we were able to reduce the induction period to around 300 s, again liberating a solvated "ligand-free" AuX_3 species. Using this precatalyst system and a specifically tailored substrate (arylthiophene **1**, Scheme 2, upper), the reaction kinetics were sufficiently tractable to allow us to determine the empirical rate law by ^{19}F NMR and to deduce that intermolecular Au(III)-arene π-complexation is the

Scheme 1. Au-Catalyzed Intermolecular Arene−Arylsilane Oxidative Coupling, As Initially Reported in 2012[5,a]

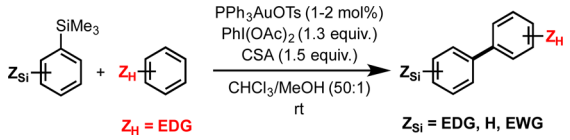

[a]CSA = camphorsulfonic acid. For further advances, see refs 6−8.

Received: September 29, 2016
Published: December 12, 2016

DOI: 10.1021/jacs.6b10018
J. Am. Chem. Soc. 2017, 139, 245−254

Scheme 2. Mechanistic Studies of Au-Catalyzed Arene–Arylsilane Oxidative Coupling[a]

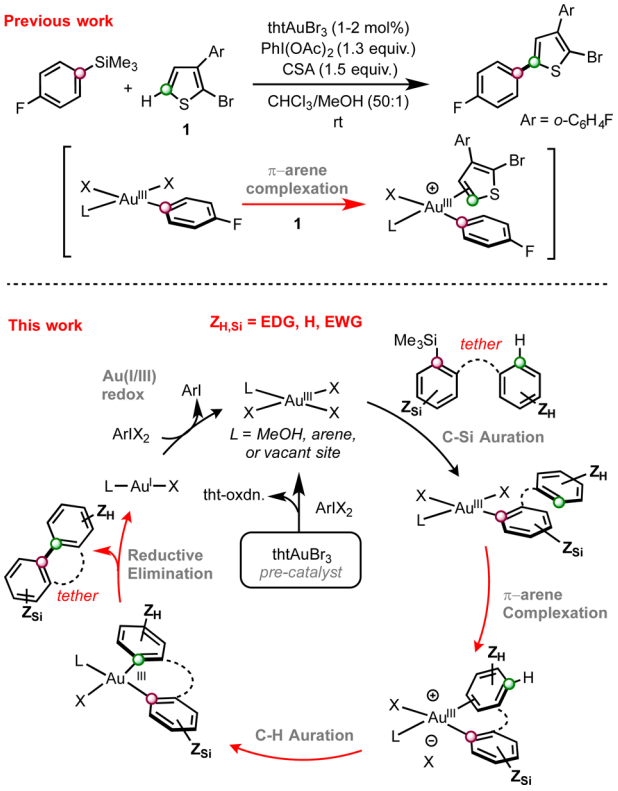

[a]tht = tetrahydrothiophene. CSA = camphorsulfonic acid. L, X = unspecified neutral and anionic ligands. The intermolecular process[9h] is limited to π-rich arenes.

turnover-limiting step (TLS).[9h] However, our conclusions were predominantly based on a detailed study of this single well-behaved model system. Information on some of the other steps in the cycle was less clear, being gained indirectly from competition experiments, literature precedent, and model stoichiometric reactions.

Gaining mechanistic insight into other steps in the cycle has become an important goal. However, to date, the process has been limited to π-rich arenes and some heterocycles. Neutral or electron-poor arenes act solely as spectators to the competing homocoupling of the aryl-trimethylsilane (aryl-TMS). This substantially limits the range of arenes that can be explored in, for example, linear free-energy relationships, even by way of analysis of relative rather than absolute rates.

Herein we report on the *intramolecular* process (Scheme 2, lower). Conducting the arylation intramolecularly induces a number of useful changes to the system: (i) in contrast to the intermolecular reaction, the reactions proceed with very reproducible and, in the main, phenomenologically simple kinetics, *vide infra*; (ii) a very broad range of arenes, including highly electron-deficient examples, can be arylated without competing arylsilane homocoupling; and (iii) the tether between the arene and the arylsilane can be used to systematically perturb arene–Au conformational flexibility, and to modulate the effective molarity of arene, in the catalytic intermediates. Overall, the intramolecular system allows substitution patterns (Z_{Si} and Z_H) and tether lengths to be tuned to provide the reactivity and kinetic regulation requisite for elucidation of mechanistic features that are *not accessible in the intermolecular version*. Using this platform, we have gained insight into arene auration, Wheland intermediate generation, and, uniquely, reductive elimination.

RESULTS AND DISCUSSION

Preparative Arylation. We began by exploring preparative cyclization, using HCIB (**2**) or PIFA (**3**) as the oxidant and the rapidly activating precatalyst thtAuBr$_3$ (*vide supra*)[9h] in CHCl$_3$/MeOH at 27 °C. A series of 35 aryl-TMS substrates (Tables 1 and 2) were cyclized, affording 5- to 9-membered rings in good to excellent isolated yields.

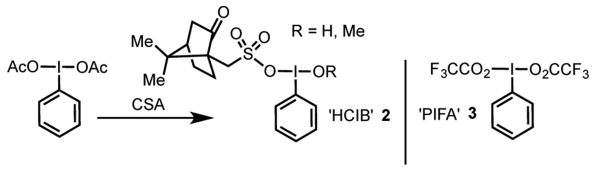

The structures of the largest rings (**5ah** and **5ai**, Table 2, entries 17 and 18) were confirmed by single-crystal X-ray diffraction. Although a number of other intramolecular direct arylation strategies have been reported,[10] the gold-catalyzed cyclization displays excellent functional group tolerance, proceeds at low reaction temperatures, uses readily prepared TMS-bearing starting materials, and yields 5- to 9-membered ring products bearing a diverse range of substituents, from *m*-CF$_3$ to *p*-OMe. For the majority of examples, 1–2 mol% Au allowed complete conversion, at 27 °C in a reasonable time scale; with some substrates, substantially lower loadings were possible. For example, cyclization of **4n** (Table 2, entry 3) was complete in under 10 min using 1 mol% Au (95% yield), and 0.06 mol% Au still afforded dimethylfluorene **5n** in 80% yield, with formal turnover number of 1330. In contrast, the cyclization of **4ah** (Table 2, entry 17) to generate 8-membered **5ah** required 4 mol% Au, and 9-membered **5ai** (Table 2, entry 18) required heating to 50 °C (52% yield). Although the formation of 8- and 9-membered rings via metal-catalyzed direct arylation has been reported,[11] examples involving simple aryl rings (no directing groups) are rare.

In some cases, in particular anisyl and naphthyl substrates **4a**, **4i**, and **4s**, the oxidant (HCIB, **2**)[12] reacts directly with the electron-rich arene to generate a diaryliodonium salt via an S_EAr mechanism.[13] This competing process, which is not Au-catalyzed, severely reduced the yield with certain examples. Changing from HCIB (**2**) to PIFA (**3**) largely eliminated diaryliodonium formation, allowing **5a**, **5i**, and **5s** to be obtained in 80–88% yields. The impact of oxidant is exemplified in the cyclization of **4a**, Table 1.

Table 1. Effect of Oxidant (2, 3) on the Cyclization of 4a

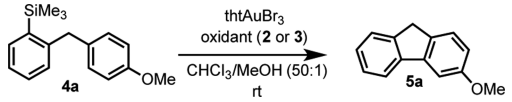

	conversion of **4a** to **5a** (%)	
thtAuBr$_3$ (mol% Au)	with HCIB (**2**)[a]	with PIFA (**3**)[b]
0.25	11	85
0.5	17	90
1	33	88
2	42	90

[a]Generated in situ from PhI(OAc)$_2$ (1.1 equiv) + CSA (1.3 equiv). [b]1.1 equiv; conversion by ^{1}H NMR using internal standard (CH_2Br_2).

DOI: 10.1021/jacs.6b10018
J. Am. Chem. Soc. 2017, 139, 245–254

Suppression of the background diaryliodonium formation using PIFA (**3**) allows substantially lower catalyst loadings to be employed.[14] The beneficial effect of replacing HCIB (**2**) with PIFA (**3**) was further explored by conversion of **6a** (X = TMS) to **7**, Scheme 3, requiring arylation of a highly electron-rich

Scheme 3. Au/Pd-Catalyzed Direct Arylation of 6a/6b[a]

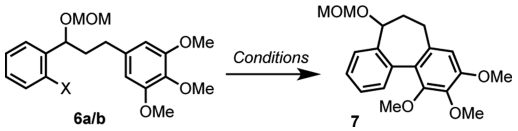

[a]Conditions: For X = $SiMe_3$ (**6a**): thtAuBr$_3$ (5 mol%), **3** (1.2 equiv), $CHCl_3$/MeOH (50:1), 2.5 h, 27 °C, 75%. For X = Cl (**6b**): $Pd(OAc)_2$ (10 mol%), K_2CO_3 (2 equiv), DMA, 14 h, 145 °C, 69%.[11f]

trimethoxybenzene ring.[15] Thus, while HCIB (**2**) led to a complex mixture, due to diaryliodonium salt generation *and* acid-mediated *in situ* MOM deprotection, use of PIFA (**3**) afforded the 7-membered ring allocolchinoid skeleton[15] **7** in 75% yield, with the MOM group intact. An analogous Pd-catalyzed process using **6b** (X = Cl) requires substantially more forcing conditions (145 °C).[11f]

Mechanistic Study. Intramolecular arylation, particularly the examples generating substituted fluorene products[16] (entries 1−8, Table 2), proved ideal for mechanistic study. First, as noted above, the intramolecular process tolerates a very much larger range of arene substituents than the intermolecular version, where only electron-rich arenes are tolerated. This key feature has allowed detailed analysis of linear free energy relationships (LFERs) for both the silane and the arene. Second, the reactions tend to proceed with reproducible and (phenomenologically) simple kinetics, often pseudo-zero-order, *vide infra*, without significant side-product formation. In contrast, the intermolecular system displays complex kinetic profiles and often suffers from competing arylsilane homocoupling. Third, deuterium labels can be readily installed at strategic positions to analyze for kinetic isotope effects (KIEs) at key steps. Finally, the tether length between the arenes is readily varied, allowing the kinetics of intramolecular arene capture to be modulated. Overall, in combination with earlier data,[9h] the system allows a more holistic analysis of the catalytic cycle.

Kinetics and Activation Parameters. In our previous investigation of the *intermolecular* reaction (Scheme 2, upper), arene π-complexation was found to be the TLS, leading to pseudo-first-order kinetics.[9h] By tethering the arene to the arylsilane, and thus in turn to the aryl-gold, the effective molarity of the arene is raised, potentially leading to the TLS being driven to another stage in the cycle. Monitoring of the reaction of **4b** by ^{1}H NMR spectroscopy revealed the expected[9h] induction period (~300 s) during which the catalyst is converted to the tht-free active species $LAuX_3$, where L = MeOH, arene, or vacant site; X = CSA, and up to one Br. After completion of the induction period, catalytic turnover proceeds with clean pseudo-zero-order kinetics, turning over for the full reaction evolution at a formal frequency of 0.07 s^{-1} at 27 °C (Figure 1, top).

The pseudo-zero-order kinetics preclude an intermolecular TLS, or an intermolecular pre-equilibrium, and thus cannot involve Au(I/III) redox by $PhIX_2$, or C−Si auration (Scheme 2). In a general sense, this confines the TLS to being one of intramolecular π-complexation, C−H auration, reductive elimination, ligand dissociation, or intracomplex reorganization/isomerization.

Eyring analysis, between 7 and 37 °C, afforded $\Delta S^{\ddagger}$ = +21 e.u. (Figure 1, lower), opposite in sign to the intermolecular arylation (Scheme 2, upper), where turnover-rate-limiting π-complexation induces a strongly negative $\Delta S^{\ddagger}$.[9h] Although interpretation of activation parameters must be done with care, the results suggest that the TLS for the *intramolecular* system occurs *after* π-complexation, which would be expected to induce a small but negative $\Delta S^{\ddagger}$. Further experiments were performed to deduce which unimolecular process, prior to bimolecular Au(I/III) redox, is turnover-rate-limiting.

Deuterium Kinetic Isotope Effects. In order to probe the C−H auration, a range of deuterated substrates were deployed in intramolecular arylation, Scheme 4, eqs 1−4. Control experiments confirmed that there is no deuterium−protium exchange before, during, or after cyclization, indicating that overall C−H/C−D cleavage is irreversible. The absolute rates of turnover of **4b** versus d_5-**4b** (Scheme 4, eq 1) were experimentally indistinguishable (k_H/k_D = 1.0). Thus, the perdeuterated phenyl ring induces no significant primary or secondary KIE on the overall rate of catalytic turnover. This eliminates C−H cleavage from consideration as the TLS.

As noted by Schmidbaur, η^2-coordination to unsaturated and aromatic hydrocarbons is the key step in gold-catalyzed organic transformations,[17] and gold(III) has a long history of interacting with arenes. For example, it has been known for over 80 years that anhydrous $AuCl_3$ reacts readily with aromatic hydrocarbons, leading to C−H auration of the arene.[18] However, to date, all attempts to experimentally prepare stable molecules demonstrating Au−arene interactions have been unsuccessful.[17] Nonetheless, such η^2-arene gold(III) π-complexes have been explored computationally[19] and are implicated as precursors to C−H auration. In our previous studies,[9h] this *intermolecular* π-complexation event was deduced to be turnover-rate-limiting, and the relative rates of arylation of a series of arenes was shown to correlate with known stabilities of reference Ag−π-arene complexes and HF/BF_3 Wheland intermediates.[9h] However, there was no indication from any of the data obtained whether steps prior to the irreversible C−H auration are reversible or not.

The reversibility of the arene π-complexation can be tested using the intramolecular cyclization. Thus, although no KIE is exhibited intermolecularly (**4b** versus d_5-**4b**), an intramolecular competition reaction employing d_1-**4b** was found to elicit a significant KIE (k_H/k_D = 2.5, Scheme 4, eq 2) on the product distribution. In order for the primary KIE arising from C−H cleavage to impact on the product distribution (**5b** versus d_1-**5b**), the isotopomeric precursor η^2-complexes (**8** and **9**, Scheme 5) must be able to equilibrate prior to irreversible, i.e., product-determining, C−H/C−D cleavage. Equilibration could occur within discrete Au−arene complexes (pathway A) or by reversible η^2-complexation (pathway B). The same primary KIE (k_H/k_D = 2.5) was obtained with bis-arene d_5-**10** (Scheme 4, eq 3), confirming that Au−arene π-complexation is reversible, with C−H/C−D cleavage being product-determining, but not turnover-rate-limiting (no KIE, Scheme 4, eq 1).

The KIEs outlined in Scheme 4, eqs 1−3, are consistent with both a concerted metalation−deprotonation (CMD) pathway[20] and an aromatic electrophilic substitution (S_EAr) pathway,[9h,18,21] both stemming from a presumed precursor η^2-complex, Scheme 5. When the methylene bridge in d_1-**4b** is

DOI: 10.1021/jacs.6b10018
J. Am. Chem. Soc. 2017, 139, 245−254

Table 2. Preparative Gold-Catalyzed Cyclizations (35 Examples) of 4a–4ai to 5a–5ai at 27 °C[a]

Entry	Substrate	Product	(Yield, Time)	Entry	Substrate	Product	(Yield, Time)
1	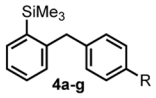 4a-g	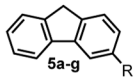 5a-g	R = OMe (88%, 2 h)[b] **5a** H (94%, 1 h) **5b** *t*-Bu (81%, 1 h) **5c** Cl (90%, 4 h) **5d** OPiv (81%, 6 h) **5e** CF_3 (80%, 15 h) **5f** OTf (92%, 16 h)[c] **5g**	10	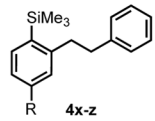 4x-z	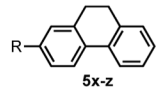 5x-z	R = H (72%, 1 h) **5x** Cl (91%, 1 h)[c] **5y** CF_3 (82%, 16 h)[c] **5z**
2	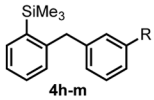 4h-m	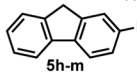 5h-m	R = Me (95%, 1 h)[d] **5h** OMe (80%, 1 h)[b,d] **5i** F (85%, 2 h)[d] **5j** Cl (90%, 3 h)[d] **5k** CF_3 (88%, 16 h)[d,e] **5l** OTf (78%, 15 h)[d] **5m**	11	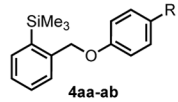 4aa-ab	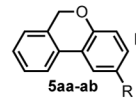 5aa-ab	R = H (86%, 2 h)[c,f] **5aa** *t*-Bu (60%, 1 h)[c,f] **5ab**
3	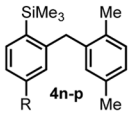 4n-p	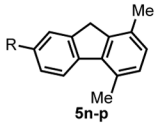 5n-p	R = H (95%, 10 min) **5n** F (89%, 15 min) **5o** Cl (91%, 1 h)[c] **5p**	12	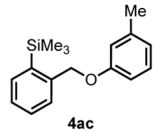 4ac	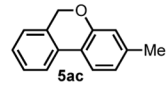 5ac	(86%, 1 h)[e,c,f]
4	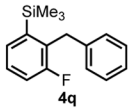 4q	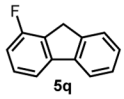 5q	(87%, 16 h)	13	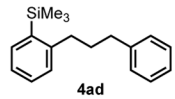 4ad	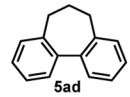 5ad	(85%, 15 h)[c]
5	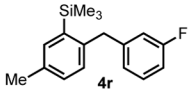 4r	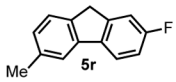 5r	(89%, 5 h)	14	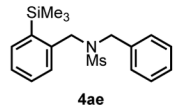 4ae	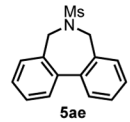 5ae	(73%, 16 h)[c]
6	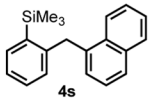 4s	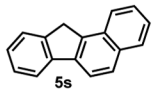 5s	(80%, 1 h)[b]	15	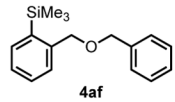 4af	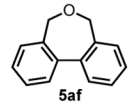 5af	(76%, 16 h)[c,e]
7	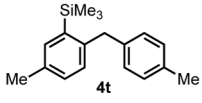 4t	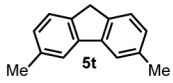 5t	(76%, 1 h)	16	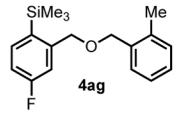 4ag	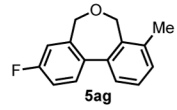 5ag	(82%, 15 h)[c]
8	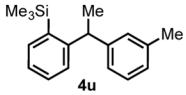 4u	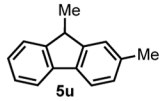 5u	(79%, 1 h)[b,c,d]	17	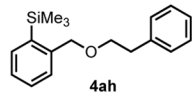 4ah	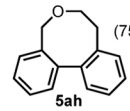 5ah	(75%, 14 h)[g] 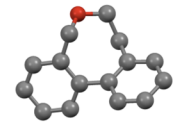
9	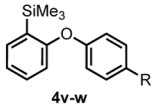 4v-w	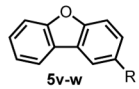 5v-w	R = H (87%, 30 min) **5v** R = CH_2NPhth (94%, 1 h) **5w**	18	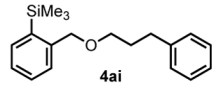 4ai	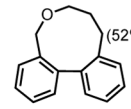 5ai	(52%, 16h)[e,g,h] 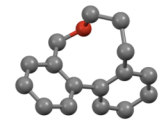

[a]Unless otherwise stated: **4** (0.50 mmol), thtAuBr$_3$ (1 mol%), PhI(OAc)$_2$ (0.55 mmol), CSA (0.65 mmol) in $CHCl_3$/MeOH (50:1, 0.1 M). [b]PhI(OCOCF$_3$)$_2$ (**3**, 0.55 mmol) replaces PhI(OAc)$_2$/CSA. [c]thtAuBr$_3$, 2 mol%. [d]Ratio of 2-/4-regioisomers: **5h** (95:5), **5i** (88:12), **5j** (97:3), **5u** (97:3); ratio of 3-/1-regioisomers: **5ac** (89:11). [e]CSA, 1.0 mmol. [f]0.05 M **4** [g]thtAuBr$_3$, 4 mol%. [h]50 °C. Phth = phthalimido. Piv = *t*-BuCO.

replaced with an *O*-atom linker, d_1-**4v**, the primary KIE is nearly eliminated (Scheme 4, eq 4), suggesting that the aryl-ether is able to sufficiently stabilize the π-complex (CMD) or the Wheland intermediate (S_EAr) such that one of these two steps, rather than the C–H/C–D cleavage, becomes product-determining.

C–H Auration via S_EAr versus CMD. Having established that, for **4b** and **10a**, C–H cleavage is irreversible and thus product-determining (Scheme 4, eqs 1–3), we studied intramolecular competition (**10b–f**) between electronically biased pairs of arenes, eq 5. This allows distinction of reaction via a monoaryl gold Wheland intermediate (S_EAr) from C–H deprotonation of a π-complex (CMD), both leading to the same diaryl gold intermediate. A large negative ρ value was obtained (ρ = −3.7; see SI). In CMD the acidity of the proton is of importance[20b] and the net (negative) inductive effects of substituents dominate, leading to a complex but overall *positive* ρ-correlation, which is not observed. In contrast, stabilizing

DOI: 10.1021/jacs.6b10018
J. Am. Chem. Soc. 2017, 139, 245–254

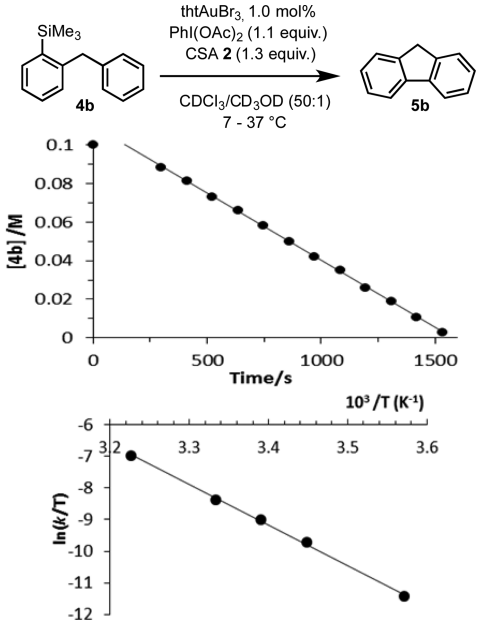

Figure 1. Top: Pseudo-zero-order kinetics for consumption of **4b** in Au-catalyzed cyclization at 27 °C; $d[\mathbf{4b}]/dt = -k_{obs}$, where $k_{obs} = k[\mathrm{Au}]$; $k = 7 \times 10^{-2}$ s^{-1}; $R^2 = 0.99$. Bottom: Eyring analysis for cyclization of **4b** (0.1 M) with 1 mol% Au, $\ln(k/T) = 34.54 - (12.86 \times 10^3/T)$; $R^2 = 1.00$; $\Delta H^{\ddagger} = +26$ kcal mol^{-1}, and $\Delta S^{\ddagger} = +21$ e.u.

Scheme 4. KIEs (Eqs 1−4) and Substituent Partitioning (Eq 5) for Intramolecular Au-Catalyzed Arylation

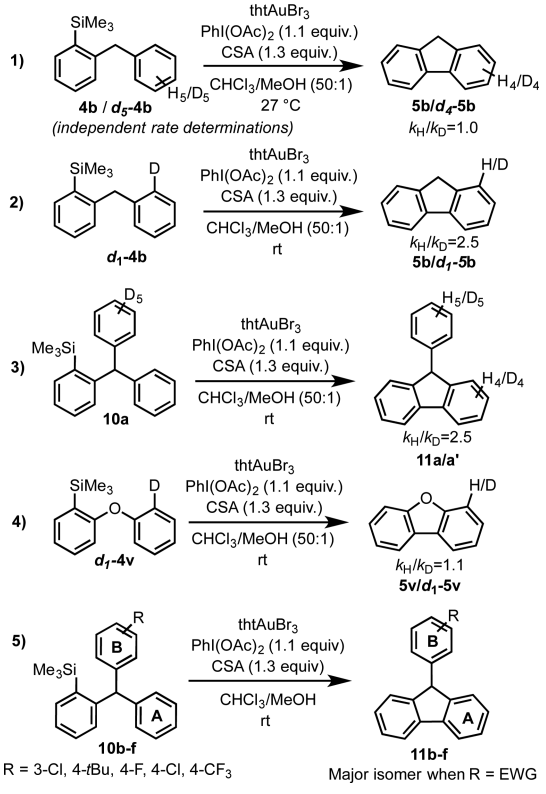

(positive) inductive and resonance effects of substituents are expected to be of importance in an S_EAr process, leading to a *negative* ρ/ρ^+-correlation.[22]

Turnover-Limiting Reductive Elimination. Reaction rates (M s^{-1}) were determined under standard conditions (0.1 M substrate, 2 mol% thtAuBr$_3$) for a series of 18 substrates in which the arene (**4a−m**) or arylsilane (iso-**4i−m**) bears a substituent that is *meta* or *para* to the site of coupling in **5a−m**, Figure 2. In addition to singly substituted substrates, bis-silyl **12** and doubly substituted **4t**/**13** were also tested. The kinetics were analyzed by way of a linear free-energy relationship (LFER) using the standard Hammett σ-function, affording a reaction constant (ρ) of −2.0.

The correlation indicates that the impact of a substituent on the rate of catalytic turnover is independent of its provenance;

Scheme 5. η^2-Arene π-Complexes and C−H Auration Mechanisms

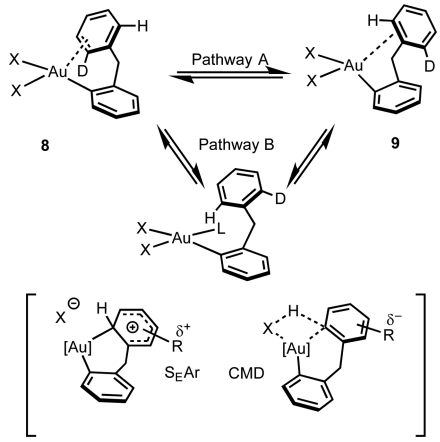

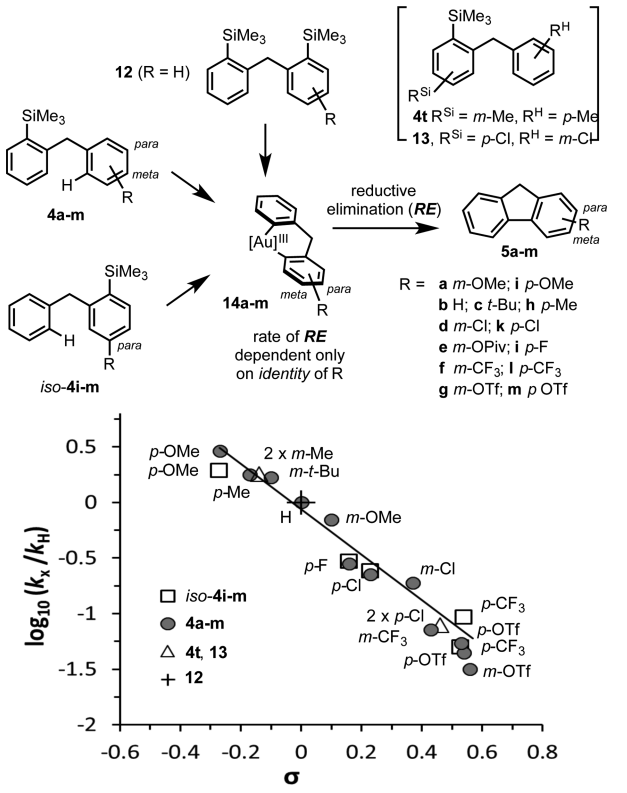

Figure 2. LFER analysis of rates of catalytic turnover during cyclization of **4a−m**; **4t**, iso-**4i−m**, **12**, and **13**; $\log_{10}(k_X/k_H) = -2.0\sigma - 0.06$;[23] σ-values are additive for **4t**/**13**. Conditions: substrate (0.05 mmol), thtAuBr$_3$ (2 mol%), 2-bromothiophene (0.5 mmol),[24] PhI(OAc)$_2$ (0.055 mmol), CSA (0.065 mmol), CDCl$_3$/CD$_3$OD (50:1, 0.1 M).

DOI: 10.1021/jacs.6b10018
J. Am. Chem. Soc. 2017, 139, 245−254

i.e. whether it was initially on the arene (**4a**–**m**), the arylsilane (iso-**4i**–**m**), or both (**4t**, **13**). This requires that the substrates converge on a common intermediate, at, or prior to, the TLS. This condition can be satisfied at any point *after* C–H cleavage to generate a diaryl-gold intermediate. Further evidence for convergence at a common intermediate arises from the identical rates of turnover of bis-TMS **12** and mono-TMS **4b** (R = H), both of which generate **5b** via reductive elimination from the same intermediate (**14b**, Figure 2, R = H). Reaction of bis-TMS **12** thus involves a *second* C–Si cleavage, rather than C–H cleavage, at the stage of the monoaryl-gold intermediate. The selective intramolecular C–Si versus C–H auration is again consistent with an S_EAr process, with TMS stabilization of the β-cation in the Wheland intermediate being favored.[9h]

The pseudo-zero-order kinetics observed for of bis-TMS **12** and mono-TMS **4b** limit the possibilities for a unimolecular TLS to reductive elimination from a diaryl-gold intermediate (**14b**), or ligand dissociation prior to this.[25] Reductive elimination is rarely the TLS in $C(sp^2)$–$C(sp^2)$ cross-coupling.[26] In most cases, oxidative addition or transmetalation is rate-limiting. Indeed, as a consequence of this, there has been a reliance on *stoichiometric* studies to indirectly investigate reductive elimination in catalytic systems.[9g,i,j,27] Details relating to the kinetics and structures involved in reductive elimination of a biaryl moiety from diaryl-gold species are very sparse. There are very few examples of isolated diaryl-gold complexes in which the aryls groups are simple, i.e., non-chelating.[9h,28] Nevado was able to isolate and characterize (X-ray)[9j,k] the neutral diaryl complex $[Ar_2Au(PPh_3)Cl]$, where Ar = C_6F_5, and found that forcing conditions were required to trigger reductive elimination of perfluorobiphenyl (150 °C, 20 h).[9j]

Pioneering studies by Kochi on trialkyl- and dialkyl-gold phosphine complexes $R_3Au(PPh_3)$ and $R_2Au(PPh_3)X$ (where R = Me, Et; X = Cl, TFA, NO_3, OTf), revealed that dissociation of PPh_3, leading to high-energy T-shaped species R_3Au and R_2AuX, precedes reductive elimination of R–R.[29] In most cases, the overall rate of reductive elimination was slow (k_{obs} = 10^{-6} to 10^{-7} s^{-1} at 45–80 °C), and the liberated PPh_3 progressively inhibited reaction by disfavoring the dissociative pre-equilibrium. The exception to this trend was $Me_2Au(PPh_3)OTf$, which reductively eliminated very rapidly (k_{obs} > 10 s^{-1} at 25 °C). The possibility of an additional pathway for reductive elimination involving triflate dissociation to generate cationic $[Me_2Au(PPh_3)]^+$ could not be discounted.[29b]

More recently, Toste has confirmed that, for specific cases, phosphine dissociation is not necessary for reductive elimination to occur.[9g] The neutral complex $[Ar_2Au(PPh_3)Cl]$, where Ar = *p*-C_6H_4F, was generated *in situ*, and found to undergo reductive elimination more efficiently (k_{obs} = 10^{-4} s^{-1} at −52 °C) than the analogous perfluoroaryl complex studied by Nevado.[9j] In contrast to the inhibiting effects of added phosphine noted by Kochi, addition of PPh_3, to generate the cationic bis(phosphine) complex $[Ar_2Au(PPh_3)_2]^+$, resulted in substantial rate enhancement (k_{obs} = 0.2 s^{-1} at −52 °C). This process is "among the fastest observed C–C bond-forming reductive couplings at any transition metal centre".[9g] The high reaction velocity is ascribed to a combination of Au(III)-destabilization by the formal cationic charge at the gold, and the driving force provided by steric decompression of the bulky triphenyl phosphine ligands as the biaryl elimination proceeds.[9g] Thus, overall, a very wide range of rates have been determined for reductive R-R elimination from gold(III) species, with a number of contributing factors, including coordination number, formal charge, steric demand of ligands, and the electron-demand by the Ar/alkyl groups undergoing elimination. The turnover rates of the intramolecular Au-catalyzed process considered herein (up to 1 s^{-1}, 27 °C, **4n**, Table 2) are significantly slower than that of the stoichiometric reductive elimination from cationic $[Ar_2Au(PPh_3)_2]^+$, but not dissimilar to that for the neutral complex $[Ar_2Au(PPh_3)Cl]$.[9g,30]

Based on the kinetic studies by Kochi,[29] the reductive elimination is expected to occur after ligand dissociation from a neutral four-coordinate precursor (**15b**, Figure 3, L =

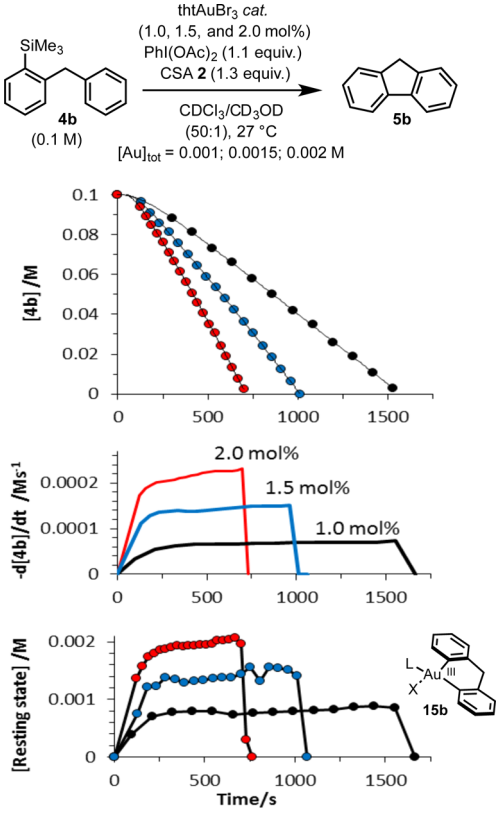

Figure 3. Top: Pseudo-zero-order kinetics (after induction period, ~300 s)[9h] for Au-catalyzed intramolecular arylation of **4b** using 1.0, 1.5, and 2.0 mol% Au. Middle: temporal turnover rate of **4b**/M s^{-1}.[31] Bottom: temporal concentration of catalyst resting state, tentatively assigned as **15b**; L = unspecified neutral ligand, e.g. arene, solvent; X = unspecified anionic ligand.

unspecified neutral ligand, e.g., arene, solvent). ^1H NMR spectroscopic analysis of the Au-catalyzed intramolecular arylation of **4b** in $CDCl_3/CD_3OD$ at 27 °C revealed a transient low-intensity methylene signal, not attributable to traces of Ph_2CH_2 or catalyst activation co-products (see SI). The signal was tentatively assigned to the $-CH_2-$ tether in **15b**. Integration against an internal standard allowed analysis of the temporal concentration of **15b**, at three different initial $thtAuBr_3$ precatalyst loadings (1.0, 1.5, and 2.0 mol%), Figure 3.

Analysis of the steady-state maximum concentration of the transient species (resting state, **15b**; Figure 3, bottom) confirmed that it accounts for >90% of $[Au]_{tot}$. Moreover, the concentration of **15b** can be correlated with the temporal changes in turnover rate (−d[**4b**]/d*t*, M s^{-1}), Figure 3, middle. Thus, during the induction period (~300 s), the concentration of **15b** rises from zero to reach the steady state, which is

DOI: 10.1021/jacs.6b10018
J. Am. Chem. Soc. 2017, 139, 245–254

maintained throughout the pseudo-zero-order phase of turnover. On complete consumption of substrate **4b**, the concentration of **15b** rapidly decays to zero.

Effect of Aryl Electron Demand and Au–Ar Conformational Mobility on Reductive Elimination Rates. The acceleration of reductive elimination by electron-donating substituents (ρ = −2.0; Figure 2) is partially consistent with literature precedent for other Ar_2[M] complexes (M = Pt, Pd), where electron-withdrawing substituents are found to strengthen the ground-state metal–carbon bonds.[27b,32] Hartwig showed, from LFER analyses, that reductive elimination from Ar_2[Pt] "is faster from complexes with a larger difference between the electron-donating properties of the two aryl groups".[27b,32] In other words, the electronic effects of substituent on reductive elimination rates *are not simply additive*. In contrast, a recent computational study on reductive elimination from *cis*-[$AuPPh_3(Ar^1)(Ar^2)$] complexes suggests that, for gold, the electronic effects of aryl substitution are additive.[33] This is now experimentally confirmed: disubstituted compounds **4t** and **13** generate diaryl-gold intermediates that reductively eliminate at rates predicted by the sum of their σ-values (Figure 2).

While most cyclizations gave pseudo-zero-order profiles (e.g., **4b**, Figure 3), the two slowest-reacting examples (*p*-CF_3 **4l**, *m*-OTf **4g**, Figure 2), where the arene ring is substituted by electron-withdrawing groups, showed distinct curvature.[34] This is indicative of turnover-rate-limiting arene π-complexation from a monoaryl-gold(III) resting state (**17**, Scheme 6),[9h] which was tested by intermolecular interception of **17l** with a π-rich arene, resulting in co-generation of biaryl **16**.[35]

Scheme 6. Dependency of Resting State Identity (15 versus 17) on the π-Complexing Ability of the Arene[a]

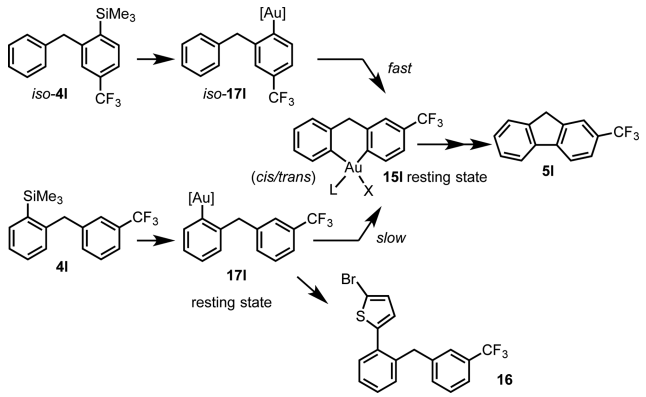

[a]Conditions: **4l**/iso-**4l** (0.05 mmol), thtAuBr$_3$ (2 mol%), PhI(OAc)$_2$ (0.055 mmol), CSA (0.065 mmol), $CDCl_3/CD_3OD$ (50:1, 0.1 M), 2-bromothiophene (0.5 mmol), 27 °C. See SI for an analysis of **5l**/**16** partitioning as a function of conversion.

Calculations on reductive elimination from unconstrained[28] [$(Ar^1)(Ar^2)Au(PPh_3)Cl$] and [$(Ar^1)(Ar^2)Au(PPh_3)$]$^+$ complexes show that the lowest energy transition state involves Au–Ar conformations in which the two aryl rings are oriented face-to-face.[33] If this arrangement is made less energetically accessible, e.g., by strain, tethering, or chelation,[28] then rates of reductive elimination will be reduced. Longer, non-rigid tethers are expected to allow greater Au–Ar conformational mobility and thus a lower energetic barrier to the attainment of the requisite face-to-face orientation of the two aryl rings. However, longer tethers will also reduce the effective molarity of the arene in the precursor C–H auration. The kinetics of cyclization of **4b** (−CH_2− tether) are distinct from those of **4x** (−CH_2CH_2− tether). In the latter case, increase of the tether length by one methylene unit results in a curved kinetic profile[34] (Figure 4), indicative of a monoaryl-gold(III) resting state.[9h]

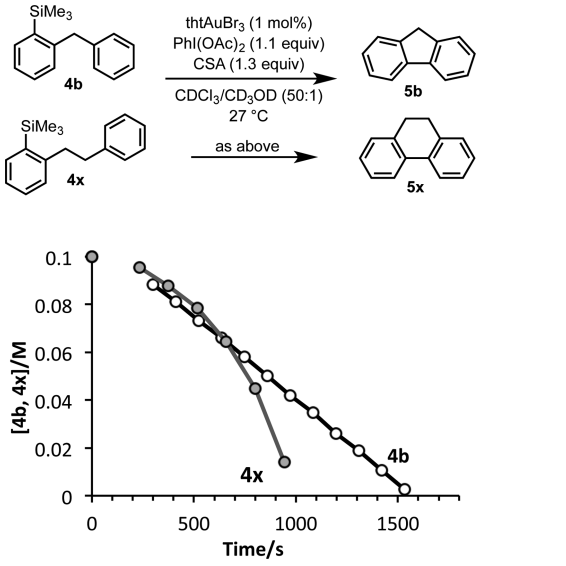

Figure 4. Turnover to generate 5- versus 6-membered rings. Initial concentration of **4b** and **4x**, 0.1 M. As the reaction proceeds, the turnover rate of **4x** accelerates,[34] becoming faster than that of **4b**.

A key observation is that, as the reaction evolves, the rate of turnover of **4x** becomes faster than that of **4b**, for which reductive elimination is turnover-rate-limiting. In other words, the intrinsic rate of reductive elimination from the longer −CH_2CH_2− tethered intermediate **14x** must be *faster* than that from the more constrained, −CH_2− tethered intermediate **14b** (Figure 5).[36]

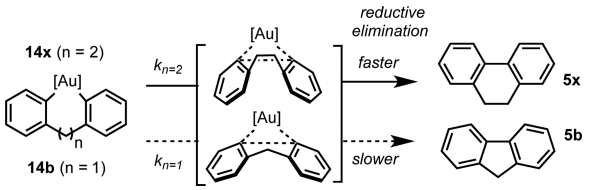

Figure 5. Effect of tether length (n) and flexibility on Ar–Au–Ar conformers from which developing Ar–Ar π-facial interaction[28,33] can facilitate reductive elimination.

A normal primary KIE of 1.9 was obtained on intramolecular competition using −CH_2CH_2− tethered d_1-**4x**, indicative that Wheland intermediate generation is partially reversible (Scheme 7). Once again, stabilization of the Wheland intermediate by replacing the a CH_2 linker by oxygen (d_1-**4aa**) eliminates the KIE. The impact of tether length (n = 1, 2) was further explored by intramolecular competition using **18** (Scheme 7). The 5-membered ring cyclization outcompetes the 6-membered ring-forming process by a factor of 13, consistent with *selectivity-determining*, i.e., irreversible, C–H cleavage after Wheland intermediate generation by ring **A**.[37]

DOI: 10.1021/jacs.6b10018
J. Am. Chem. Soc. 2017, 139, 245–254

Scheme 7. KIEs for 6-Membered Ring Cyclization of 4x and 4aa, and Intramolecular Competition (A versus B) To Generate 5-Membered (19) versus 6-Membered (20) Rings

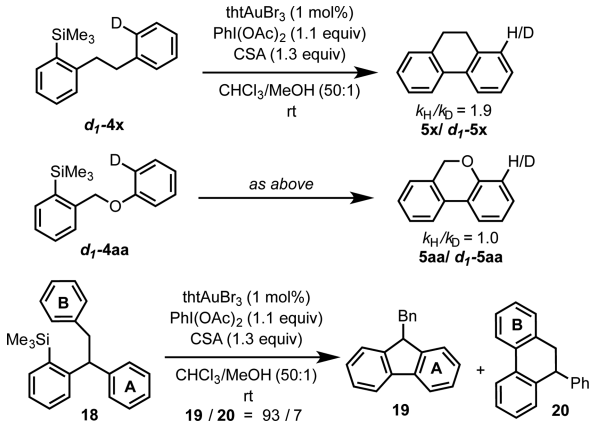

Scheme 8. Mechanism of Au-Catalyzed Intramolecular Arylation (4 → 5) with Turnover-Rate-Limiting Step (TLS) Proceeding from a Mono-aryl- (17) or Di-aryl-gold (15) Resting State, Depending on Tether Length (*n*) and Electronic Influence of Arene Substituent (R^2)[a]

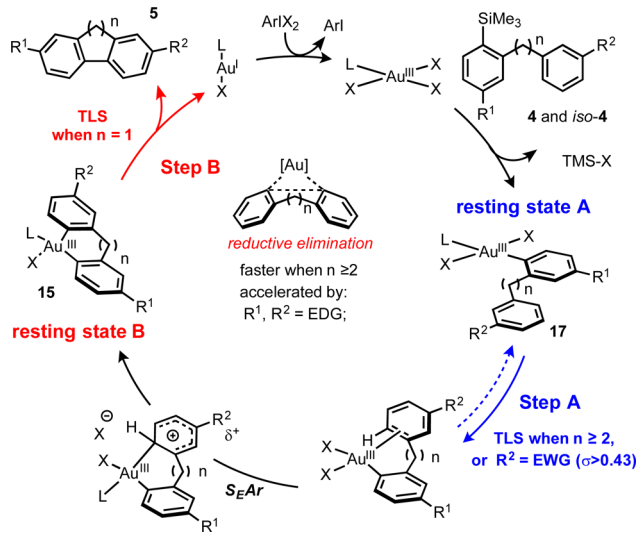

[a]L = unspecified ligand: arene, solvent. X = CSA, Br. For reductive elimination, L = vacant site (**14**).

CONCLUSIONS

In 2012, we introduced a gold-catalyzed intermolecular direct arylation reaction that uses arylsilanes to catalytically generate highly electrophilic Ar–Au intermediates capable of arylating arenes at ambient temperature.[5] The reaction has proven to be a high-yielding, mild, and efficient process for the coupling of a wide variety of arylsilanes with electron-rich arenes and heteroarenes.[5−8] Herein we have studied the intramolecular version of the arylation, both as a preparative process and as a vehicle for mechanistic study. Using a standard set of conditions, 44 examples of annelated biaryls, with ring sizes ranging from 5- to 9-membered, including heteroatoms and a diverse range of arene substituents, have been prepared under mild conditions at ambient temperature (Table 2, Schemes 4 and 7).[38] While the majority of the reactions proceed with minimal side-product generation, some highly electron-rich substrates are susceptible to a competing direct reaction with the $ArIX_2$ oxidant (HCIB, **2**) to generate diaryliodonium salts. In such cases, PIFA (**3**) can be used as a milder reagent to attenuate this undesired oxidation. This effect is unique to the intramolecular process and facilitates the clean arylation of even highly electron-rich arenes, such as the trimethoxybenzene moiety of the allocolchinoid skeleton **7**,[15] Scheme 3.

Rendering the arylation process intramolecular induces a number of changes that facilitate mechanistic investigation. First, unlike the intermolecular system, the vast majority of the intramolecular substrates undergo turnover with simple and reproducible kinetics, without complications from side reactions such as arene oxidation or arylsilane homocoupling. Second, only electron-rich arenes can be arylated intemolecularly, limiting the range of arene substituents that can be explored in linear free-energy relationships. In contrast, the intramolecular system tolerates a wide range of arene substituents, both electron-donating and electron-withdrawing, and the kinetics have been determined for substituents with σ-values ranging from −0.3 to +0.6. Third, relative to all of the other Au(III)-mediated steps[39] in the intermolecular catalytic cycle, reductive elimination from diaryl-gold(III) is fast. Consequently, it has not previously been possible to acquire kinetic data for this key C–C bonding-forming process. Application of the intramolecular system has been pivotal in this regard. It allows two effects to be used in concert: (a) tethering the arene to the arylsilane induces high effective molarity and raises the velocity of the C–H auration step, while (b) close-tethering of the aryls decreases the velocity of the reductive elimination. In certain cases these two effects have been sufficient to move the catalyst resting state to the diaryl-gold(III) intermediate, allowing a detailed analysis of the influence of substituents on the rate of reductive elimination.

Using the unique features of the intramolecular variant of the arylation process, we have been able to elucidate the following:

(i) ^{2}H kinetic isotope effects (Schemes 4 and 7) support our previous conclusion[5,9h] that the C–H auration involves aromatic electrophilic substitution (S_EAr)[21] via a Wheland intermediate, rather than a concerted metalation–deprotonation (CMD) pathway.[20]

(ii) When the aryl-arene tether is $-CH_2CH_2-$, despite the high effective molarity of the arene, the C–H auration, beginning with step **A** (Scheme 8), is the turnover-rate-limiting step.[9h]

(iii) Reduction of the tether length from $-CH_2CH_2-$ to $-CH_2-$ results in a migration of the turnover-rate-limiting step from **A** to **B**, Scheme 8, but only when the arene is sufficiently π-complexing ($\sigma \leq 0.43$).

(iv) Reductive elimination from a diaryl-gold(III) intermediate generates the biaryl product **5** (step **B**) and is accelerated by electron-donating substituents (R^1, R^2) on the aryl rings. The effect is independent of whether the substituent was originally on the arylsilane or the arene ring. The acceleration correlates with standard σ-values for R^1, R^2, and if both rings are substituted, the effect is additive ($\sigma_{net} = \sigma\text{-}R^1 + \sigma\text{-}R^2$).

(v) There is a requirement for a face-to-face arrangement[33] of the two aryl rings during reductive elimination (step **B**). The shorter $-CH_2-$ tether results in a slower rate of reductive elimination compared to the longer $-CH_2CH_2-$ unit, as the latter allows greater conforma-

DOI: 10.1021/jacs.6b10018
J. Am. Chem. Soc. 2017, 139, 245−254

tional freedom for the system to attain the required arrangement of the two aryl rings.

In summary, the investigation of catalytic reaction mechanism plays an important role in the discovery and development of new synthetic methodology. It can lead to useful generalizations and design principles in the optimization and application of catalysis. However, mechanistic studies are often limited to a small collection of well-behaved substrates or constrained to a narrow range of accessible reaction conditions. In such cases, mechanistic insight must be extrapolated with caution, even for what may appear to be a closely related system: the assumption that the same parameters and constraints apply may not be valid. The results presented herein demonstrate exactly such a situation. Even small changes in the substrate structure lead to different mechanistic behaviors. Thus, by changing a single aryl substituent from being above or below $\sigma = 0.43$, or by varying the tether length by one methylene unit, the catalyst resting state can switch from one side of the cycle to the other (**A** versus **B**, Scheme 8). The last step of the cycle, the Au(I)/Au(III) redox by $ArIX_2$ reagents (e.g., **2** and **3**), remains one for which very little mechanistic detail is known. Rapid redox is essential for the success of the reaction;[39] this process is under active investigation.

■ ASSOCIATED CONTENT

Supporting Information

The Supporting Information is available free of charge on the ACS Publications website at DOI: 10.1021/jacs.6b10018.

Additional discussion, experimental procedures, kinetic data, characterization data, and NMR spectra (PDF)

X-ray crystallographic data for **5ah** (CIF)

X-ray crystallographic data for **5ai** (CIF)

■ AUTHOR INFORMATION

Corresponding Author

*guy.lloyd-jones@ed.ac.uk

ORCID

Guy C. Lloyd-Jones: 0000-0003-2128-6864

Notes

The authors declare no competing financial interest.

■ ACKNOWLEDGMENTS

The research leading to these results has received funding from the European Research Council under the European Union's Seventh Framework Programme (FP7/2007-2013)/ERC grant agreement no. 340163.

■ REFERENCES

(1) (a) *Metal-Catalyzed Cross-Coupling Reactions and More*; de Meijere, A., Bräse, S., Oestreich, M., Eds.; Wiley-VCH Verlag GmbH & Co.: Weinheim, Germany, 2014. (b) Johansson Seechurn, C. C. C.; Kitching, M. O.; Colacot, T. J.; Snieckus, V. *Angew. Chem., Int. Ed.* **2012**, *51*, 5062−5085. (c) Hassan, J.; Sévignon, M.; Gozzi, C.; Schulz, E.; Lemaire, M. *Chem. Rev.* **2002**, *102*, 1359−1470.

(2) Hussain, I.; Singh, T. *Adv. Synth. Catal.* **2014**, *356*, 1661−1696.

(3) For reviews on direct arylation, see: (a) Liu, C.; Yuan, J.; Gao, M.; Tang, S.; Li, W.; Shi, R.; Lei, A. *Chem. Rev.* **2015**, *115*, 12138−12204. (b) Yamaguchi, J.; Yamaguchi, A. D.; Itami, K. *Angew. Chem., Int. Ed.* **2012**, *51*, 8960−9009. (c) Ackermann, L. *Chem. Rev.* **2011**, *111*, 1315−1345. (d) Lyons, T. W.; Sanford, M. S. *Chem. Rev.* **2010**, *110*, 1147−1169. (e) Ackermann, L.; Vicente, R.; Kapdi, A. R. *Angew. Chem., Int. Ed.* **2009**, *48*, 9792−9826. (f) McGlacken, G. P.; Bateman, L. M. *Chem. Soc. Rev.* **2009**, *38*, 2447−2464.

(4) For reviews on gold catalysis, see: (a) Pflasterer, D.; Hashmi, A. S. K. *Chem. Soc. Rev.* **2016**, *45*, 1331−1367. (b) Zi, W.; Toste, F. D. *Chem. Soc. Rev.* **2016**, *45*, 4567−4589. (c) Zheng, Z.; Wang, Z.; Wang, Y.; Zhang, L. *Chem. Soc. Rev.* **2016**, *45*, 4448−4458. (d) Dorel, R.; Echavarren, A. M. *Chem. Rev.* **2015**, *115*, 9028−9072. (e) Deharo, T.; Nevado, C. *Synthesis* **2011**, *2011*, 2530−2539. (f) Wegner, H. A.; Auzias, M. *Angew. Chem., Int. Ed.* **2011**, *50*, 8236−8247. (g) Hashmi, A. S. K. *Chem. Rev.* **2007**, *107*, 3180−3211. (h) Jimenez-Nunez, E.; Echavarren, A. M. *Chem. Commun.* **2007**, *4*, 333−346. (i) Hashmi, A. S. K.; Hutchings, G. J. *Angew. Chem., Int. Ed.* **2006**, *45*, 7896−7936.

(5) Ball, L. T.; Lloyd-Jones, G. C.; Russell, C. A. *Science* **2012**, *337*, 1644−1648.

(6) Hata, K.; Ito, H.; Segawa, Y.; Itami, K. *Beilstein J. Org. Chem.* **2015**, *11*, 2737−2746.

(7) Hua, Y.; Asgari, P.; Avullala, T.; Jeon, J. *J. Am. Chem. Soc.* **2016**, *138*, 7982−7991.

(8) Cresswell, A. J.; Lloyd-Jones, G. C. *Chem. - Eur. J.* **2016**, *22*, 12641−12645.

(9) For reviews on reactivity and isolation of gold complexes, see: (a) Joost, M.; Amgoune, A.; Bourissou, D. *Angew. Chem., Int. Ed.* **2015**, *54*, 15022−15045. (b) Hashmi, A. S. K. *Angew. Chem., Int. Ed.* **2010**, *49*, 5232−5241. For selected recent advances in the field, see: (c) Kawai, H.; Wolf, W. J.; DiPasquale, A. G.; Winston, M. S.; Toste, F. D. *J. Am. Chem. Soc.* **2016**, *138*, 587−593. (d) Joost, M.; Estévez, L.; Miqueu, K.; Amgoune, A.; Bourissou, D. *Angew. Chem., Int. Ed.* **2015**, *54*, 5236−5240. (e) Winston, M. S.; Wolf, W. J.; Toste, F. D. *J. Am. Chem. Soc.* **2015**, *137*, 7921−7928. (f) Wu, C.-Y.; Horibe, T.; Jacobsen, C. B.; Toste, F. D. *Nature* **2015**, *517*, 449−454. (g) Wolf, W. J.; Winston, M. S.; Toste, F. D. *Nat. Chem.* **2014**, *6*, 159−164. (h) Ball, L. T.; Lloyd-Jones, G. C.; Russell, C. A. *J. Am. Chem. Soc.* **2014**, *136*, 254−264. (i) Wu, Q.; Du, C.; Huang, Y.; Liu, X.; Long, Z.; Song, F.; You, J. *Chem. Sci.* **2015**, *6*, 288−293. (j) Hofer, M.; Gomez-Bengoa, E.; Nevado, C. *Organometallics* **2014**, *33*, 1328−1332. (k) Hofer, M.; Nevado, C. *Eur. J. Inorg. Chem.* **2012**, *2012*, 1338−1341.

(10) For pioneering studies into intramolecular direct arylation, see: (a) Lafrance, M.; Lapointe, D.; Fagnou, K. *Tetrahedron* **2008**, *64*, 6015−6020. (b) Campeau, L. C.; Parisien, M.; Jean, A.; Fagnou, K. *J. Am. Chem. Soc.* **2006**, *128*, 581−590. (c) Campeau, L. C.; Parisien, M.; Leblanc, M.; Fagnou, K. *J. Am. Chem. Soc.* **2004**, *126*, 9186−9187.

(11) For select examples of 7-, 8-, and 9-membered ring synthesis via direct arylation, see: (a) Pintori, D. G.; Greaney, M. F. *J. Am. Chem. Soc.* **2011**, *133*, 1209−1211. (b) Majumdar, K. C.; Ray, K.; Ganai, S. *Tetrahedron Lett.* **2010**, *51*, 1736−1738. (c) Blaszykowski, C.; Aktoudianakis, E.; Alberico, D.; Bressy, C.; Hulcoop, D. G.; Jafarpour, F.; Joushaghani, A.; Laleu, B.; Lautens, M. *J. Org. Chem.* **2008**, *73*, 1888−1897. (d) Beccalli, E. M.; Broggini, G.; Martinelli, M.; Paladino, G.; Rossi, E. *Synthesis* **2006**, *2006*, 2404−2412. (e) Bressy, C.; Alberico, D.; Lautens, M. *J. Am. Chem. Soc.* **2005**, *127*, 13148. (f) Leblanc, M.; Fagnou, K. *Org. Lett.* **2005**, *7*, 2849−2852. (g) Bowie, A. L.; Hughes, C. C.; Trauner, D. *Org. Lett.* **2005**, *7*, 5207−5209. (h) Kozikowski, A. P.; Ma, D. *Tetrahedron Lett.* **1991**, *32*, 3317.

(12) Hatzigrigoriou, E.; Varvoglis, A.; Bakola-Christianopoulou, M. *J. Org. Chem.* **1990**, *55*, 315−318.

(13) For a review on synthesis and application of diaryliodonium salts, see: Merritt, E. A.; Olofsson, B. *Angew. Chem., Int. Ed.* **2009**, *48*, 9052−9070.

(14) Increased yields are obtained only with the most electron-rich substrates. PIFA (**3**) does not lead to productive catalysis in intermolecular examples, presumably because it does not release a strong enough acid (such as CSA) to catalyze the methanol dissociation for π-complexation/C−H auration.[9h]

(15) For examples of syntheses of this scaffold, see: (a) Djurdjevic, S.; Yang, F.; Green, J. R. *J. Org. Chem.* **2010**, *75*, 8241−8251. (b) Besong, G.; Jarowicki, K.; Kocienski, P. J.; Sliwinski, E.; Boyle, F. T. *Org. Biomol. Chem.* **2006**, *4*, 2193−2207. (c) Vorogushin, A. V.; Predeus, A. V.; Wulff, W. D.; Hansen, H. J. *J. Org. Chem.* **2003**, *68*, 5826−5831.

DOI: 10.1021/jacs.6b10018
J. Am. Chem. Soc. 2017, 139, 245−254

(16) For a recent review on transition-metal-catalyzed synthesis of fluorenes, see: Zhou, A.-H.; Pan, F.; Zhu, C.; Ye, L.-W. *Chem. - Eur. J.* **2015**, *21*, 10278−10288.
(17) Schmidbaur, H.; Schier, A. *Organometallics* **2010**, *29*, 2−23.
(18) Kharasch, M. S.; Isbell, H. S. *J. Am. Chem. Soc.* **1931**, *53*, 3053−3059.
(19) Ghosh, M. K.; Tilset, M.; Venugopal, A.; Heyn, R.; Swang, O. *J. Phys. Chem. A* **2010**, *114*, 8135−8141.
(20) For mechanistic studies on the CMD mechanism with palladium, see: (a) Gorelsky, S. I.; Lapointe, D.; Fagnou, K. *J. Org. Chem.* **2012**, *77*, 658−668. (b) García-Cuadrado, D.; de Mendoza, P.; Braga, A. A. C.; Maseras, F.; Echavarren, A. M. *J. Am. Chem. Soc.* **2007**, *129*, 6880−6886. For a perspective on CMD in general, see: (c) Lapointe, D.; Fagnou, K. *Chem. Lett.* **2010**, *39*, 1118−1126. For a perspective on CMD with Pd, see: (d) Livendahl, M.; Echavarren, A. M. *Isr. J. Chem.* **2010**, *50*, 630−651.
(21) For stoichiometric studies on the S_EAr/CMD mechanisms for gold, see: (a) Kharasch, M. S.; Beck, T. M. *J. Am. Chem. Soc.* **1934**, *56*, 2057−2060. (b) Liddle, K. S.; Parkin, C. *J. Chem. Soc., Chem. Commun.* **1972**, 26. (c) de Graaf, P. W. J.; Boersma, J.; van der Kerk, G. J. M. *J. Organomet. Chem.* **1976**, *105*, 399−406. (d) Fuchita, Y.; Utsunomiya, Y.; Yasutake, M. *J. Chem. Soc., Dalton Trans.* **2001**, 2330−2334. (e) Rosca, D.-A.; Smith, D. A.; Bochmann, M. *Chem. Commun.* **2012**, *48*, 7247−7249. (f) Hofer, M.; Nevado, C. *Tetrahedron* **2013**, *69*, 5751−5757. (g) Cambeiro, X. C.; Boorman, T. C.; Lu, P.; Larrosa, I. *Angew. Chem., Int. Ed.* **2013**, *52*, 1781−1784. Under catalytic conditions, see: (h) Cambeiro, X. C.; Ahlsten, N.; Larrosa, I. *J. Am. Chem. Soc.* **2015**, *137*, 15636−15639. See also ref 9h.
(22) A "normal" ρ value would be expected for π-complexation, whereas a ρ^+ value would be expected for Wheland intermediate generation; see ref 9h. The KIEs obtained with **10a** indicate π-complexation is reversible for simple phenyl rings. However, the rate data do not give an ideal linear correlation, and the electronically biased rings in **10b−f** may shift the process away from Curtin−Hammett control such that the ratios begin to reflect the equilibrium population.
(23) Standard Hammett σ-values were employed (Hansch, C.; Leo, A.; Taft, R. W. *Chem. Rev.* **1991**, *91*, 165−195.) except for the value for *p*-F where, in our experience, $\sigma_p = 0.15$ (Shulgin, A. T.; Baker, A. W. *Nature* **1958**, *182*, 1299.) is better parameterized for reactions in non-aqueous media, as compared to the standard value of $\sigma_p = 0.06$, which was determined in water.
(24) Kinetic profiles obtained with electron-deficient arylsilanes were partially nonlinear; this was resolved by addition of 2-bromothiophene. The detailed kinetics of this phenomenon are currently under investigation. Arenes **4l** (*p*-CF_3) and **4g** (*m*-OTf) also gave curved kinetic profiles (i.e., imperfect pseudo-zero-order kinetics) that were not linearized by addition 2-bromothiophene. The rate averages were employed for the correlation and are slightly lower than predicted by $\log_{10}(k_X/k_H) = -2.0\rho - 0.06$. See Figure 2 and associated text for more detailed discussion, and SI for rate limits.
(25) The large $\Delta S^{\ddagger}$ value (Figure 1) may be an *apparent* activatiton parameter, arising from combination of a pre-equilibrium dissociation with irreversible reductive elimination from a three-coordinate intermediate.
(26) (a) Jin, L.; Zhang, H.; Li, P.; Sowa, J. R.; Lei, A. *J. Am. Chem. Soc.* **2009**, *131*, 9892−9893. (b) Amatore, C.; Jutand, A. *Organometallics* **1988**, *7*, 2203−2214.
(27) (a) Osakada, K.; Onodera, H.; Nishihara, Y. *Organometallics* **2005**, *24*, 190−192. (b) Shekhar, S.; Hartwig, J. F. *J. Am. Chem. Soc.* **2004**, *126*, 13016−13027. (c) Merwin, R. K.; Schnabel, R. C.; Koola, J. D.; Roddick, D. M. *Organometallics* **1992**, *11*, 2972−2978. (d) Braterman, P. S.; Cross, R. J.; Young, G. B. *J. Chem. Soc., Dalton Trans.* **1977**, 1892−1897.
(28) Reductive elmination from chelated Ph−Au(X)−(Ar-*N*-donor) complexes requires addition of PPh_3 to displace the *N*-donor: Vicente, J.; Dolores Bermudez, M.; Escribano, J. *Organometallics* **1991**, *10*, 3380−3384. See also ref 9g.
(29) (a) Komiya, S.; Albright, T. A.; Hoffmann, R.; Kochi, J. K. *J. Am. Chem. Soc.* **1976**, *98*, 7255−7265. (b) Komiya, S.; Kochi, J. K. *J. Am. Chem. Soc.* **1976**, *98*, 7599−7607. (c) Tamaki, A.; Magennis, S. A.; Kochi, J. K. *J. Am. Chem. Soc.* **1974**, *96*, 6140−6148.
(30) Use of the reported activation parameters (ref 9g) for $Ar_2Au(PPh_3)Cl$ indicates that the rate of reductive elimination of this system at 27 °C is about 5 s^{-1}.
(31) Turnover rates were estimated by differentiation of high-order polynomial fits to the temporal concentration plots.
(32) Hartwig, J. F. *Inorg. Chem.* **2007**, *46*, 1936−1947.
(33) (a) Nijamudheen, A.; Karmakar, S.; Datta, A. *Chem. - Eur. J.* **2014**, *20*, 14650−14658.
(34) Rates for these substrates are dependent on the CSA concentration, see SI, which rises as oxidant (**2**) is consumed. The curvature does not arise from a longer induction period; precatalyst activation is complete in around 300 s[9h] (based on analysis of Ar-Br coproducts, see SI), this being less than 2% of the time taken for complete turnover of the substrate.
(35) Control experiments confirmed that the pseudo-zero-order rate profile for cyclization of iso-**4l** is *independent* of CSA concentration, consistent with turnover of iso-**4l** via reductive elimination from the normal diaryl gold (**15l**) resting state. For systems bearing a $-CH_2-$ tether, the transition from di- to monoaryl-gold resting state is only observed for examples **4l** and **4g**, where the arene ring bears strongly electron-withdrawing groups ($\sigma_{net} \geq 0.43$). Bromothiophene-trapped products were not obtained with any substrates where $\sigma_{net} < 0.43$.
(36) At this stage we cannot assess how much faster the reductive elimination to the 6-membered ring is, as the change in kinetic profile also suggests a change in the TLS; thus, turnover rate may be limited by π-complexation or reductive elimination, or both, at different stages in the reaction evolution.
(37) This selectivity may arise from the differential developing strain in 6-membered versus 7-membered aurocycles generated from rings **A** and **B**, respectively.
(38) This applies to all but **4ai** (Table 2, entry 18), which required heating to 50 °C.
(39) If the Au(I)X/Au(III)X_3 redox is not sufficiently rapid (due to low oxidant concentration or kinetically ineffective oxidant species), then the Au(I) disproportionates, resulting in rapid catalyst deactivation.

DOI: 10.1021/jacs.6b10018
J. Am. Chem. Soc. 2017, 139, 245−254